Magnetic Response of Metamaterials at 100 Terahertz

Stefan Linden, *et al.*

Science **306**, 1351 (2004);
DOI: 10.1126/science.1105371

Magnetic Response of Metamaterials at 100 Terahertz

Stefan Linden,[1] Christian Enkrich,[2] Martin Wegener,[1,2] Jiangfeng Zhou,[3] Thomas Koschny,[3,4] Costas M. Soukoulis[3,4]*

An array of single nonmagnetic metallic split rings can be used to implement a magnetic resonance, which arises from an inductor-capacitor circuit (LC) resonance, at 100-terahertz frequency. The excitation of the LC resonance in the normal-incidence geometry used in our experiments occurs through the coupling of the electric field of the incident light to the capacitance. The measured optical spectra of the nanofabricated gold structures come very close to the theoretical expectations. Additional numerical simulations show that our structures exhibit a frequency range with negative permeability for a beam configuration in which the magnetic field couples to the LC resonance. Together with an electric response that has negative permittivity, this can lead to materials with a negative index of refraction.

Our ability to tailor the potential of electrons on the scale of their de Broglie wavelength has opened the door to new frontiers in nanoelectronics. Similarly, our ability to tailor the index of refraction of materials is the route to new avenues in nanophotonics. Usually, the index of refraction n determines the factor to which the propagation of light in a medium is slower than in vacuum. Hence, one traditionally expects n to be a positive number. Most of the time, n is larger than unity. With this in mind, the recently realized metamaterials (*1*), which have a negative index of refraction (*2*–*6*), came as a surprise to many. The negative n in these so-called left-handed materials (*2*) can lead to new physical phenomena and potential applications, such as "perfect lenses" (*3*).

Under conditions of negative refraction, a light wave impinging from vacuum or air onto the metamaterial's surface under an angle with respect to the surface normal is refracted toward the "wrong" side of the normal (*1*). A negative index of refraction, n, in Snell's law indeed reproduces this unusual behavior. Mathematically, the square of the index of refraction, $n^2 = \varepsilon\mu$, is given by the product of the electric permittivity ε and the magnetic permeability μ of the medium. If both permittivity and permeability are negative, the resulting refractive index is negative as well. A negative permittivity is not unusual and occurs in any metal from zero frequency to the plasma frequency; however, a large magnetic response, in general, and a negative permeability at optical frequencies, in particular, do not occur in natural materials.

It is of particular importance to terahertz optics and their applications (*7*) to achieve magnetic resonant response at terahertz and higher frequencies. In metamaterials, this crucial aspect is achieved by mimicking an LC oscillator of eigenfrequency ω_{LC} with $\omega_{LC} = (LC)^{-1/2}$, consisting of a magnetic coil with inductance L and a capacitor with capacitance C (Fig. 1). The incident light can couple to the LC resonance (*8*), if at least one of the following conditions is fulfilled (Fig. 1): (i) The electric field vector $\boldsymbol{E}$ of the incident light has a component normal to the plates of the capacitor, or (ii) the magnetic field vector $\boldsymbol{H}$ of the incident light has a component normal to the plane of the coil. If condition (ii) is fulfilled, the current in the coil, analogous to an atomic orbital current, leads to a magnetic field that counteracts the driving magnetic field, which can lead to a negative permeability. Such metamaterials were first realized at frequencies around 10 GHz (3-cm wavelengths) (*1*, *9*) and could be fabricated on stacked electronic circuit boards.

It was believed that corresponding materials at optical frequencies, which are more than four orders of magnitude higher (a few hundred terahertz), were out of reach because of Ohmic losses. However, microstructures with magnetic resonance frequencies that were two orders of magnitude larger at about 1 THz (300-μm wavelength) were recently fabricated by microlithography (*10*). Using nanofabrication techniques, we increased the LC-resonance frequency by yet another two orders of magnitude to about 100 THz (3-μm wavelength), bringing optical frequencies into reach for obtaining negative index of refraction. Both transmission and reflection were measured. The measured transmission spectra gave more than 90% transmission, so the losses are relatively low for these very thin metallic structures. The comparison of the measured optical spectra with theory shows very good agreement.

Our design of the structures closely follows a recent theoretical suggestion (*8*), which uses single split-ring resonators (SRRs) rather than double SRRs (*1*, *10*). We used periodic quadratic arrays of such SRRs made from gold with the dimensions given by the electron micrographs shown in Fig. 1 and on the right-hand side of Fig. 2. All samples discussed have an area of 25 by 25 μm. For example, a lattice constant of a = 450 nm corresponds to a total number of 56 × 56 = 3136 SRRs (see supporting online material text for fabrication and characterization details).

Figure 2 summarizes a number of different spectroscopic results in the form of a "matrix." Electron micrographs of corresponding samples are shown together with illustrations of the two linear polarization configurations used in the measurements. All of the lattice constants (from 450 to 900 nm) are much smaller than the 3-μm LC-resonance wavelength, discussed in the experiments and calculations below.

After the illustration in Fig. 1, the magnetic field vector of the incident light has a vanishing component normal to the coil for normal incidence conditions. Thus, coupling to the LC resonance is only possible if the electric field vector has a component normal to the plates of the capac-

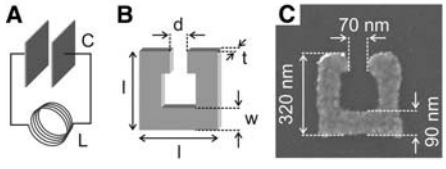

Fig. 1. Illustration of the analogy between a conventional LC circuit (**A**), consisting of an inductance L, a capacitance C, and the single SRRs used here (**B**). l, length; w, width; d, gap width; t, thickness. (**C**) An electron micrograph of a typical SRR fabricated by electron-beam lithography. The thickness of the gold film is t = 20 nm. For normal incidence, where the magnetic field vector $\boldsymbol{B}$ lies in the plane of the coil, the electric field vector $\boldsymbol{E}$ of the incident light must have a component parallel to the electric field of the capacitor to couple to the LC circuit. This allows the coupling to be controlled through the polarization of the incident light (Fig. 2).

[1]Institut für Nanotechnologie, Forschungszentrum Karlsruhe in der Helmholtz-Gemeinschaft, D-76021 Karlsruhe, Germany. [2]Institut für Angewandte Physik, Universität Karlsruhe (TH), Wolfgang-Gaede-Straße 1, D-76131 Karlsruhe, Germany. [3]Ames Laboratory and Department of Physics and Astronomy, Iowa State University, Ames, Iowa 50011, USA. [4]Institute of Electronic Structure and Laser (IESL), Foundation for Research and Technology-Hellas (FORTH), 71110 Heraklion, Crete, Greece.

*To whom correspondence should be addressed. E-mail: soukoulis@ameslab.gov

itance (*8*), which corresponds to the left column of spectra in Fig. 2. For all lattice constants, *a*, two distinct resonances are clearly visible. Their spectral position does not depend on *a*. With increasing lattice constant *a*, the resonances narrow to some extent because of the reduced interaction between the SRRs, but their spectral position remains essentially unchanged, as expected for the electric and magnetic resonant responses of SRRs (*6*). The long-wavelength resonance around 3-μm wavelength completely disappears if the electric field vector is rotated by 90° (right column of spectra in Fig. 2). This is expected for the LC resonance, according to our above reasoning (Fig. 1). Also, see the more thorough theoretical discussion in (*8*). To further strengthen our interpretation of the 3-μm resonance in terms of an LC resonance, we show corresponding spectra for closed rings (*6*) rather than split rings in Fig. 2, G and H. Indeed, the 3-μm resonance does not occur for either linear polarization in this case, and the reflection and transmission spectra are nearly identical for the two polarizations, apart from minor deviations, because of imperfections in the nanofabrication process.

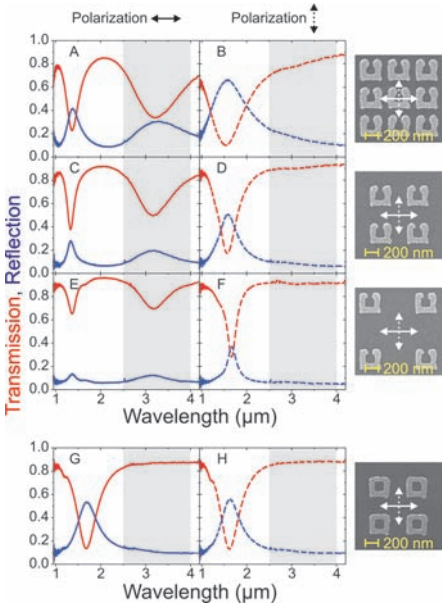

Fig. 2. Measured transmission (red) and reflection (blue) spectra. In each row of this "matrix," an electron micrograph of the sample is shown on the right-hand side. The two polarization configurations are shown on top of the two columns. In the first row (**A** and **B**), the lattice constant of the SRRs is a = 450 nm; in the second row (**C** and **D**), it is a = 600 nm; and in the third row (**E** and **F**), it is a = 900 nm. (A) to (F) correspond to nominally identical SRRs. In the last row (**G** and **H**), results for closed-ring resonators with a = 600 nm are shown. The combination of these spectra unambiguously shows that the resonance at about 3-μm wavelength (highlighted by the gray areas) is the LC resonance of the individual SSRs.

The additional transmission minimum between 1- and 2-μm wavelengths is due to the electric resonance arising from the currents induced by the electric field of the incident radiation in the metallic sides of the SRR. These currents are parallel to the polarization of the electric field. This electric resonance is related to the plasmon resonance in a thin continuous wire but shifted to nonzero frequency as a result of the additional depolarization field arising from the finite side length of the SRR. It appears independent of the excitation of the circular currents of the LC resonance and also occurs for the closed rings (Fig. 2, G and H). This electric resonance is sometimes also referred to as the particle-plasmon resonance. Finally, we have performed measurements (*11*) under an angle of up to 40° with respect to the surface normal, such that the magnetic field vector of the incident light acquires a component normal to the coils [similar to (*10*)]. As expected, the 3-μm resonance persists and does not shift. Larger angles of incidence are not possible in our experiments because of geometrical restrictions of the microscope used and because of the limited depth of focus.

To further strengthen our above assignment of the peaks and to determine the implications for possible left-handed materials, we compared these measurements with theory. In these calculations, the actual geometrical parameters (Fig. 1B) of the experiment were used. The calculations were performed with the software package CST Microwave Studio (Computer Simulation Technology GmbH, Darmstadt, Germany). The Drude model is used to describe the metal. That is, the effective permittivity of metals in the infrared spectral region is given by

$$\varepsilon(\omega) = 1 - \frac{\omega_p^2}{\omega(\omega + i\omega_c)}$$

where ω_p is the plasma frequency and ω_c is the collision frequency. For bulk gold, the parameters are $\omega_p = 2\pi \times 2.175 \times 10^{15}$ s^{-1} and $\omega_c = 2\pi \times 6.5 \times 10^{12}$ s^{-1} (*12*). For the thin gold films of our SRR, we expected that electrons experience additional scattering resulting from the metal surfaces. Thus, we used a value that is 1.65 times as large for the scattering frequency than in bulk. This obviously increases the absorption and improves the agreement between simulated and experimental observed losses. Numerical results are shown in Fig. 3, which can be directly compared with the experiment (Fig. 2). The overall agreement is very good. In particular, the absolute spectral positions of the peaks are reproduced with better than 10% accuracy. Furthermore, the polarization dependence (e.g., compare Fig. 3, A and B) also agrees with the experiment. Importantly, the resonance around 3-μm wavelength disappears for the closed rings (e.g., compare Fig. 3, C and G). According to our above reasoning, such behavior is indeed expected for the

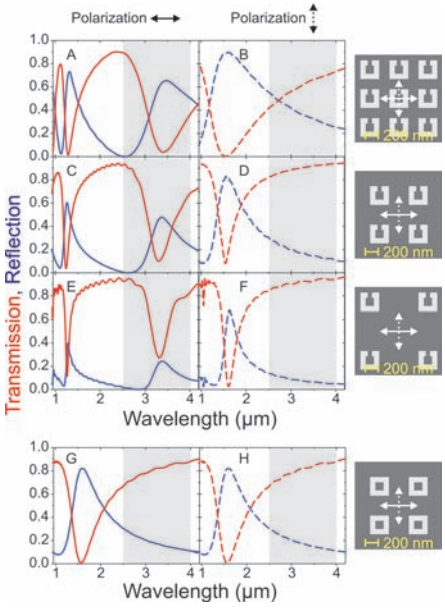

Fig. 3. (**A** to **H**) Calculated transmission (red) and reflection (blue) spectra, corresponding to the experiments shown in Fig. 2.

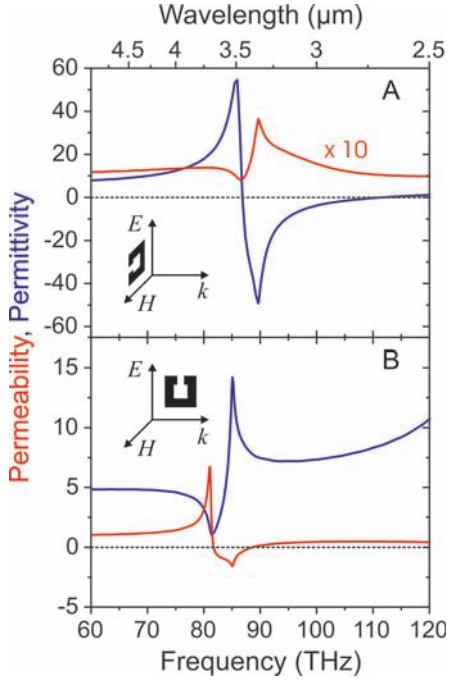

Fig. 4. The real part of the retrieved effective permeability μ and permittivity ε around the LC resonance of the SRR for the case of purely electric coupling (**A**) and purely magnetic coupling (**B**). In (A), μ has been multiplied by a factor of 10 to improve visibility. A negative μ region is observed for magnetic coupling (B). The resonance/antiresonance coupling between ε and μ is due to the periodic structure of the metamaterial (*14*). *E*, electric field vector; *H*, magnetic field vector; *k*, wave vector.

magnetic resonance, because the incident electric field cannot couple to the capacitance of the LC circuit. This argument is also true for the vertical polarization.

Figure 4 shows the effective permeability μ and the effective permittivity ε around the LC resonance, retrieved from the computed scattering data for two different orientations of the SRRs with respect to the incident wave (*13*). Figure 4A corresponds to the spectra shown on Fig. 3A, where only the electric field can couple to the LC resonance (*8*). In this case we obtain an electric resonant response in ε, accompanied by a simultaneous antiresonant behavior in μ (*14*). The retrieved data for the other polarization (Fig. 3B) exhibits no structure in ε and μ in this frequency range (*11*). In Fig. 4B, the beam configuration is such that the magnetic field can couple to the LC resonance, whereas the electric field cannot. For this polarization, a magnetic resonant response in μ is obtained with a negative value of μ in the 85-THz region. This is an important precondition for the realization of a metamaterial with a negative index of refraction. The retrieved ε exhibits an antiresonant behavior in this case (*14*).

Our results have two important consequences. First, usual ferromagnetic and antiferromagnetic resonances tend to die out above gigahertz frequencies. Thus, one can usually safely assume that the magnetic permeability of optical materials is unity. In other words, the optical properties of materials are exclusively determined by the optical polarization; the optical magnetization is zero. This is no longer true for the metamaterials presented here, enabling interesting new effects in linear optics as well as in nonlinear optics. Indeed, additional theoretical calculations show that the local fields within the gap of the LC circuit can be orders of magnitude larger than in free space or in bulk, which potentially enhances nonlinear effects and conversion efficiencies considerably. Second, a negative magnetic permeability would allow for negative-index materials at optical frequencies, which seemed totally out of reach just a few years ago.

References and Notes

1. R. A. Shelby, D. R. Smith, S. Schultz, *Science* **292**, 77 (2001).
2. V. G. Veselago, *Sov. Phys. Usp.* **10**, 509 (1968).
3. J. B. Pendry, *Phys. Rev. Lett.* **85**, 3966 (2000).
4. D. R. Smith, W. J. Padilla, D. C. Vier, S. C. Nemat-Nasser, S. Schultz, *Phys. Rev. Lett.* **84**, 4184 (2000).
5. D. R. Smith, S. Schultz, P. Markos, C. M. Soukoulis, *Phys. Rev. B* **65**, 195104 (2002).
6. T. Koschny, M. Kafesaki, E. N. Economou, C. M. Soukoulis, *Phys. Rev. Lett.* **93**, 107402 (2004).
7. C. Sirtori, *Nature* **417**, 132 (2002).
8. N. Katsarakis, T. Koschny, M. Kafesaki, E. N. Economou, C. M. Soukoulis, *Appl. Phys. Lett.* **84**, 2943 (2004).
9. D. R. Smith, J. B. Pendry, M. C. K. Wiltshire, *Science* **305**, 788 (2004).
10. T. J. Yen *et al.*, *Science* **303**, 1494 (2004).
11. S. Linden *et al.*, data not shown.
12. M. A. Ordal *et al.*, *Appl. Opt.* **22**, 1099 (1983).
13. D. R. Smith, S. Schultz, P. Markos, C. M. Soukoulis, *Phys. Rev. B* **65**, 195104 (2002).
14. T. Koschny, P. Markos, D. R. Smith, C. M. Soukoulis, *Phys. Rev. E* **68**, 065602 (2003).

15. We acknowledge the support by the Center for Functional Nanostructures (CFN) of the Deutsche Forschungsgemeinschaft (DFG) within project A.1.4. The research of M.W. is further supported by the DFG-Leibniz award 2000 and that of C.M.S. by the Alexander von Humboldt senior-scientist award 2002, by Ames Laboratory (contract no. W-7405-Eng-82), European Union Future and Emerging Technologies project, Development and Analysis of Left-Handed Metamaterials, and Defense Advanced Research Projects Agency (contract no. MDA 972-01-2-0016).

Supporting Online Material

www.sciencemag.org/cgi/content/full/306/5700/1351/DC1
SOM Text

17 September 2004; accepted 20 October 2004

A Chiral Route to Negative Refraction

J. B. Pendry

Negative refraction is currently achieved by driving the magnetic permeability and electrical permittivity simultaneously negative, thus requiring two separate resonances in the refracting material. The introduction of a single chiral resonance leads to negative refraction of one polarization, resulting in improved and simplified designs of negatively refracting materials and opening previously unknown avenues of investigation in this fast-growing subject.

Negative refraction is an intriguing and counterintuitive phenomenon that has attracted much attention. Not only does light bend the "wrong" way at a normal/negative interface, but there are even more surprising properties, such as the ability to construct a "perfect" lens for which the resolution is limited not by the wavelength but by the quality of manufacture (*1*, *2*). Negative refraction never occurs in nature, and we rely on artificial materials, metamaterials, to realize the effect as discussed in (*3*). In this paper, I discuss the consequences of chirality and show that it offers an alternative to the present routes to negative refraction. I produce a practical design that is chiral, has many advantages, and exhibits novel properties.

In the original description of negative refraction (*4*), it was stated that when the electrical permittivity and magnetic permeability are both negative light bends the wrong way at an interface. It was only much later, with the ability to construct artificial metamaterials, that the properties could be realized (*5*–*7*): The original prescription for a subwavelength array of thin metallic wires combined with resonant metallic rings has been extensively investigated, and negative refraction at microwave frequencies has been confirmed by several investigators (*8*–*13*). Although referred to as "left-handed" materials, I stress that the sense in which this term was used has nothing to do with chirality. Therefore I prefer to use the expression "negatively refracting" to avoid confusion.

The nonchiral designs suffer some limitations. They use two sets of resonant structures, one for the electric and the other for the magnetic response, and these structures have to be very carefully designed to resonate in the same frequency range. Figure 1 shows a typical schematic band structure where it was assumed that

$$\mu < 0, \omega_1 > \omega > \omega_3$$
$$\varepsilon < 0, \omega_2 > \omega > \omega_4 \quad (1)$$

where μ is the magnetic permeability, ω is the frequency, and ε is the effective electric permittivity. The negatively dispersing band between ω_2 and ω_3 is responsible for a negative refractive index. The structure of the metamaterial is required to be as fine as possible so that the fields experience an effectively homogeneous material. The pres-

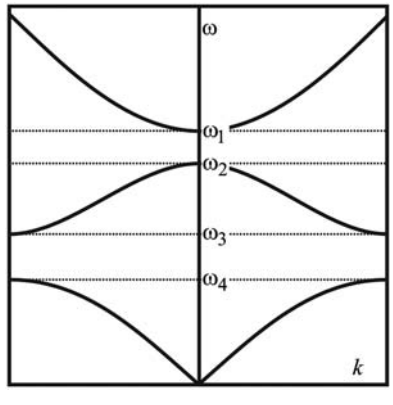

Fig. 1. Dispersion in a negatively refracting material: Typically two stop bands, $\omega_1 > \omega > \omega_2$ and $\omega_3 > \omega > \omega_4$, and a band of negative dispersion and hence of negative refraction, $\omega_2 > \omega > \omega_3$, are seen. In addition, there are two longitudinal modes (not shown), one magnetic in character and the other electric.

Department of Physics, Blackett Laboratory, Imperial College London, London SW7 2AZ, UK.